International Journal of Engineering Inventions
ISSN: 2278-7461, www.ijeijournal.com
Volume 1, Issue 9 (November2012) PP: 01-08

CFD Computation of Educator Diffuser System with Multi Lobed Nozzle

Dr.B.Balakrishna[1], G.Sankara Rao[2]
[1]*Associate professor, Department of mechanical engineering, University College of engineering, JNTU Kakinada, A.P, INDIA.*
[2]*PG student, Department of mechanical engineering, University College of engineering, JNTU Kakinada, A.P, INDIA.*

Abstract:—To prepare educator diffuser model by using CATIAV5R20.This device works on the principle that the plume temperatures can be brought down by mixing ambient air with exhaust gases and the uptake metal surface temperature can be reduced by insulating the uptake metal from the exhaust gases through formation of thin film of ambient air entrained at each diffuser ring. In this paper, the IRSS device has been redesigned by putting multi lobed nozzles in place of simple circular nozzle, expecting an enhancement in the gas cooling phenomenon. The 4, 6,8,10 lobed design of nozzle has been attempted taking into consideration of the back pressure restrictions and manufacturing feasibility. The analysis has shown a complicated phenomenon occurring inside the modified device having some positive effects in bringing down the plume temperature along with some adverse effects. Comparative analysis for different dimensions has also been carried out to choose a better design of 4 lobed nozzles [1-4]

Keywords:—CATIA, Educator diffuser, Fluent, Gambit, ICEMCFD, Multilobednozzle.

I. INTRODUCTION

The name means below red, the Latin infra meaning "below". Red is the color of the longest wavelengths of visible light. Infrared light has a longer wavelength (and so a lower frequency) than that of red light visible to humans, hence the literal meaning of below red. An infrared source can be described by the spectral distribution of power emitted by an ideal body (a black body curve). Infrared detectors are based either on the generation of a change in voltage due to a change in the detector temperature resulting from the power focused on it, or on the generation of a change in voltage due to some photon-electron interaction in the detector material. This latter effect is sometimes called the internal photo electric effect. Infrared radiation, electromagnetic radiation having a wavelength in the range from c. 75×10^{-6} cm to c.100, 000×10^{-6} cm (0.000075-0.1 cm). Infrared rays thus occupy that part of the electromagnetic spectrum with a frequency less than that of visible light and greater than that of most radio waves, although there is some overlap. Infrared radiation is thermal, or heat, radiation [10-12]. It was first discovered in 1800 by Sir William Herschel, who was attempting to determine the part of the visible spectrum with the minimum associated heat

II. LITERATURE REVIEW SHIP IR SIGNATURE OVERVIEW

A ship signature is made up from two main components: [13-16] internally generated, and externally generated. Internally generated signature sources include rejected heat from engines and other equipment, exhaust products from engines, waste air from ventilation systems and heat losses from heated internal spaces. The primary internal IR source results from the main machinery onboard any vessel, in particular drive engines and electrical generators. The magnitude of signatures produced by other sources such as heated windows, weapon systems, and deck mounted machinery is insignificant in comparison if main machinery is not suppressed. Externally generated sources result from the surfaces of a ship absorbing and/or reflecting radiation received from its surroundings. The primary sources of background radiation are: the sun, sky radiance, and sea radiance. Effective IR suppression of a ship must consider both sources [6]. Some argue that there is no point to suppressing the internally generated sources (plumes, uptakes, hot spots) because it is not possible to suppress the external sources. This ignores the fact that there is no solar heating at night or when the sky is overcast. It also ignores the fact that the sun also generates clutter. With some active measures such as water wash, the external sources can be taken care of to some degree.

III. IR RADIATION SOURCES IN NAVEL SHIP

There are three major IR sources in naval ship. These are exhaust plume, duct surfaces, hull and associated surfaces. Exhaust plume emit strongly only in 3-5 μm range, hull emits in 8-12 μm range, while duct surfaces emit radiation in both ranges. For avoiding the ship to become point target, exhaust gases and duct surfaces are to be cooled to near ambient. The Birk and Davis [3] made a simple calculation of IR signature on a hypothetical ship. The Calculation of plume radiation has accounted for radiation attenuation
by atmospheric CO_2 as described by Birk and Davis[5].. The following section describes a number of ways in which the metal and plume signatures can be reduced.

Source	Temperature (°C)	Effective area (m^2)
Hull	20	1500
Plume	400	20
Visible ducting	400	5

Table1: presents assumed temperatures and area
Used in the analysis

IV. PRINCIPLE OF OPERATIONS OF AIR EDUCTOR DIFFUSER*:*

Air eductor diffuser type of IRSS devices works on the principle that the plume temperature can be brought down by mixing of ambient air with exhaust gases and the uptake metal surface temperature can be reduced by insulating the uptake metal from hot exhaust gases through formation of thin film of ambient air entrained at each diffuser ring.

4.1 IR DETECTION:

According to the IR/EO Handbook [9], there are three basic types of detection pertinent to target acquisition modeling: Detection: a temporally unconstrained perception of an object at a specific display field location.
Pure detection: detection where the two alternative choices are (1) that something is present or (2) that nothing is present. Discrimination detection: a detection where the two alternative choices are (1) the object is a target or (2) the object is something else, such as a natural scene element. Traditionally, the target acquisition process is broken up into two distinct parts: Search tasks: the position of the target is unknown, and the time to locate the target is of fundamental importance [4]. The process of IR detection used by NTCS is a static performance measure based on pure detection. .Among the all offline control methods proposed above Tyreus-Luyben PID controller tuning and Lag/Lead compensators gives better output response whenever the disturbance occurred in the system the response is degrades as shown in the table1. Because the offline control methods are designed with fixed algorithms. To avoid this limitation an online controller is proposed for controlling the attitude of the longitudinal autopilot for general aviation aircraft based on Artificial Neural Networks.

V. IR SUPPRESSION SYSTEM:

Typically, suppression system cools the exhaust duct surfaces by film cooling and plume by mixing of naturally injected ambient air with hot plume. The above figure shows the schematic of Eductor/Diffuser IR suppression system. Figure 1 shows a number of systems currently in use for engine IRSS [9]. Further, due to negative pressure inside the device, ambient air is sucked through ring gaps and creates an ambient air film over duct surfaces, thus cools the duct surfaces within 20-30 deg Celsius of ambient. The negative pressure inside the device gets recovered and become ambient pressure at the end of the device.

5.1 COOLING AIR INJECTION FOR PLUME COOLING:

A large quantity of ambient air-cooling is required to provide a significant reduction in the average exhaust plume temperature. Such quantity of air is usually introduced using an eductor type device as shown in figure. Eductors typically consist of a suction chamber of plume, a driving nozzle, a mixing tube and a diffuser as shown in figure. For ship applications the suction chamber is usually some space within the funnel and air reaches this space through funnel-mounted louvers. The primary gas stream (in this the exhaust gases) is accelerated through the primary nozzle and is vented in the mixing tube. The resulting jet entrains air from the suction chamber. The two fluids mix in the mixing tube. The combined flow is decelerated in the diffuser to recover kinetic energy from the steam. The diffuser need not to be present if it is not desired to reduce the kinetic energy in the combined flow.

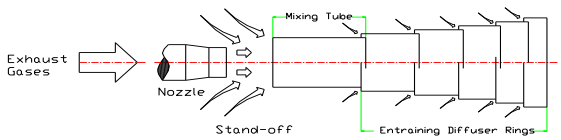

Figure 1: *Educator/ Diffuser Device*

(1) The uniformness of the temperature profile at the exit of the device (i.e. the degree of mixing between the primary gas streams the secondary cooling air stream)
(2) The requested back pressure applied on the engines to obtain a given pumping rate. One other important performance item is the resulting jet noise created the device. For a further discussion of noise effects reader is directed to Birk and Davis.

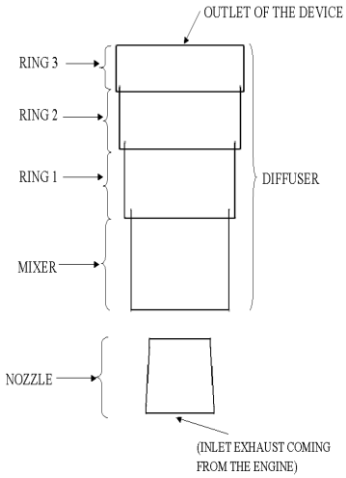

Figure 2: *The performance of an eductor system used for IRSS measured by Its ability to pump cool air.*

Extensive research has been conducted to establish design data for eductors, otherwise known as jet pumps or ejectors. The device consists of nozzle, mixing tube and a set of diffuser rings.. Typically for IRSS hard ware applications the gas flows are incompressible (i.e. Mach numbers less than 0.3) and highly turbulent (red grater then 200000.

5.2 PERFORMANCE CHARACTERISTICS:

After the preliminary design is over, CFD is employed in evaluating IRSS device performance using Finite Volume

The basic steps involved in CFD analysis are :

(i) Pre-processing.
(ii) Solving.
(iii) Post processing.

Pre-processing: This consists of preparation of CAD model, preparation of meshed model, applying boundary conditions, specifying turbulent parameters, flow parameters and control parameters etc. [7-9]

Solving: The problem is solved iteratively by CG method. Post processing: Software will generate plots of various parameters, like static pressure, temperature, velocity, density etc. These plots helps in studying the effect of film cooling on cooling exhaust duct surfaces, effect of mixing on plume temperature distribution at device exit.

VI. BACK GROUND EFFECTS:

The IR signature of a ship cannot be considered without accounting for the background in which it resides. For a seeker to locate and track a ship, the ship must appear different than its background.[17-20]

The appearance of the background depends on a number of factors including:

i) Solar disk radiation;
ii) Solar scatter by the atmosphere (dust, aerosols);
iii) Solar reflection/scatter from clouds;
iv) Solar reflection from sea surface;
v) Solar interference (shadows) from clouds; and
vi) Sky and path radiation.

6.1 DISCRETIZATION:

The discretization procedure approximate the space and time derivatives of the flow variable at each node to algebraic functions of the values of the variables at the given node and a selection of its neighbors is done through the four principal strategies that can be adopted to do this. These are

1. The Finite Difference Method
2. The Finite Volume Method.
3. The Finite Element Method.
4. The Spectral Method

.

6.2 DESCRIPTION ABOUT PLOTS:

XY PLOT: XY plot are two-dimensional plots. They represent the variation of one dependent variable vs. other independent variable a disadvantage of XY plot is they usually do not illustrate the global nature of set of CFD result all in one view.

CONTOUR PLOT: A contour line is a line along which some property is constant generally contour are plotted to an adjacent contour line is held constant.

VECTOR PLOT: A vector plot is a display of a vector quantity at discrete grid points, showing both magnitude and direction, when the base of each vector located at the respective grid point.

SCATTER PLOT: In a scatter plot a symbol is drawn at discrete grid points in the flow.

6.3 BASIC STEPS INVOLVED IN CFD ANALYSIS:

1. Geometry
2. Physics
3. Mesh
4. Solve
5. Post processing

VII. MODELING OF THE IRSS DEVICE:

CATIA V5 R16 was used for modeling the IRSS device. The steps followed for modeling is discussed as below. First we selected the start option in the main menu and choose the mechanical design and then part design. In this step we have selected the revolution surface definition command as shown in the above figure and revolved the wire frame model into 360^0 with respect to z-axis. After revolution create the surfaces at inlet and outlet of each ring, mixing tube and nozzle, by using fill command in the surface modeling. For entering in to surface modeling select start command in utility menu and choose it.

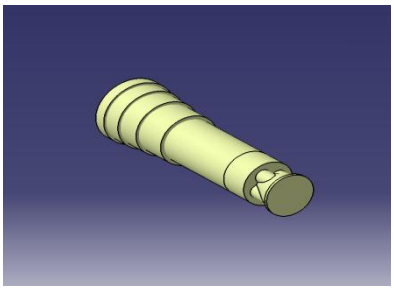

Figure 3: *Surfaces Filling*

The boundary conditions are taken as two times of the diameter (i.e. 2400 mm) and three times of the length (i.e. 12000 mm). To draw the boundary circle at the inlet of the nozzle create a new plane by using plane option in wire frame modeling window. And then create one more plane at exit of the device and draw a circle on that plane. The figure shows the boundary circles and planes. The boundary conditions are very important to find the variation of the temperature, pressure and velocity in atmosphere. How those are changed in atmospheric conditions and how much quantity has absorbed by atmosphere.

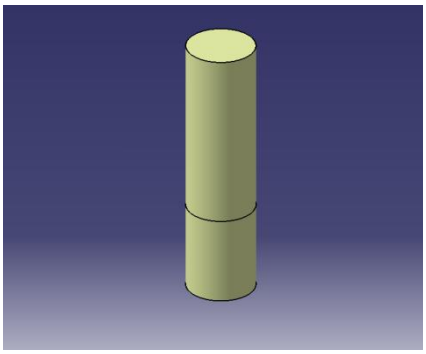

Figure 4: *Surface with Boundary Model of IRSS Device*

After creating the boundary circles select the boundary circle at nozzle inlet and extrude it up to the boundary length limit (i.e. 12000mm).

7.1 MESHING FOR IRSS DEVICE:

The ICEM CFD 5.1 is the mesh tool. It is used to create the hexa or tetra meshing. It can import model from IDEAS, CATIA etc. In this case we have generated the model with CATIA and then imported it to ICEM. In the utility window of this screen options like file, geometry, meshing etc. are shown. To import the catia model we have to go like this. By using this procedure we can import the geometry from CATIA.

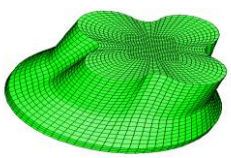

Figure 5: *lobed nozzle*

The above figures shows the wire frame meshed model of device, solid meshed model of the device and also meshed models of different types of lobed nozzles. The entire meshing process is represented in the form of flow chart as shown in figure (6.9). The mesh is generated in the following manner after that the saving of the mesh model is done and then the meshed model is exported to STAR CD.

Figure 6: *Mesh Model of the Device*

After giving all the input parameters before giving the run command save the model file, geometry file, and problem file. And then apply run star interactively command, the iterations of the problems starts and ends until the problem converges at a particular value and displays on screen the solution is converged. The entire flow analysis process is shown in the form of flow chart in the figure

VIII. ANALYTICAL RESULTS

The thermal and flow plots have been obtained for a 4 lobed nozzle. The root diameter of the nozzle is 402mm and lobe diameter is 250mm. The first figure shows the effect of lobed nozzle on the thermal distribution pattern viewed from the top at a section near the top ring. The peak value being 324.5°C Second Figure is a thermal pattern of mixing tube. The bottom part is comparatively cool because of suction of atmospheric air from the plenum.,5^{th},6^{th} plots are showing the temperature of 2^{nd} ,3^{rd},4^{th} metal rings respectively, under the influence of film cooling by cool ambient air and the turbulent mixing of gas and secondary air. Their peak temperatures are well within the desired limit. So alone peak temperature cannot depict the mixing efficiency .Average temperature is also required and for this structure it is 155 °C. Another important aspect is the pumping capacity of the device i.e. the amount of secondary air gets sucked in at the plenum area and through the annular slots. For the inlet hot mass of 7.46 Kg/sec, 5.82 Kg/sec cold air entered into the mixing chamber and all total of 17.65 Kg/sec gas expelled into the atmosphere.

8.1 PLOTS FOR 4 LOBED NOZZLE RESULTS:

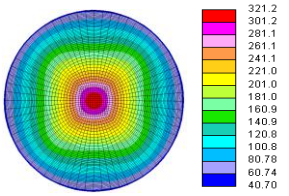

A. Plume Peak Temperature

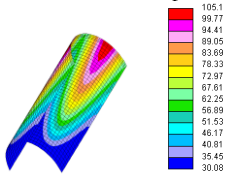

B. Mixer

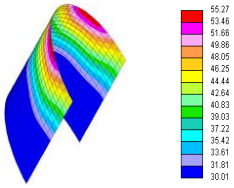

C. Ring 1

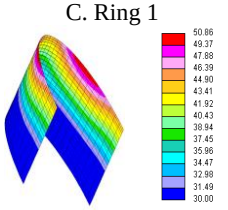

D. Ring2

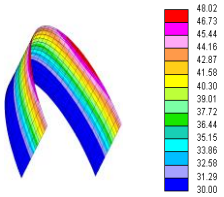

E. Ring 3

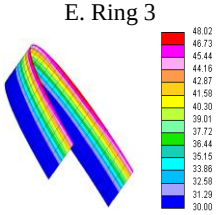

F. Ring 4

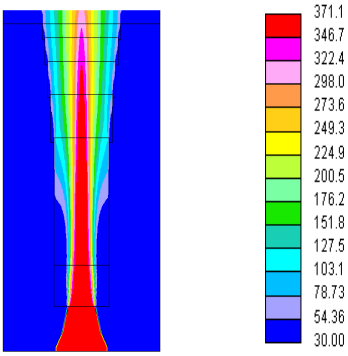

G. PlumeTemperature

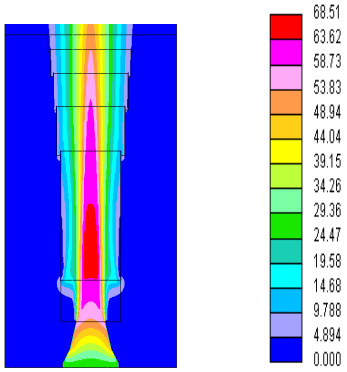

H. Plume Velocity

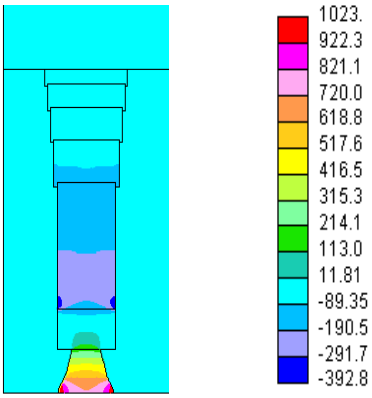

I. Static Pressure

AVERAGE PLUME TEMPERATURE : 155 °C

MASS FLUX RATE AT MIXER ENTRY : 13.41Kg/sec

MASS FLUX RATE AT DEVICE EXIT : 17.62 Kg/sec

Figures 7: *[A-I] Plots for 4 Lobed Nozzles*

Models	Maximum Metal Temperature					Peak plume temperature	Average plume temperature	Mass flux at device exit	Mass flux at mixer exit
	Mixer tube	Ring1	Ring2	Ring3	Ring4				
Circular nozzle	66.79	50.82	47.77	46.10	41.75	354.5	164.00	17.22	12.93
4lobed BASE=430 LOBE=230	107.0	55.43	51.72	48.89	44.30	318.8	151.93	17.61	13.39
4lobed BASE=416 LOBE=241	105.1	55.27	50.86	48.02	43.58	371.1	155.48	17.62	13.41
4lobed BASE=402 LOBE=250	104.3	54.74	49.11	45.77	41.83	324.5	155.97	17.65	13.28
4lobed BASE=390 LOBE=258	102.7	55.80	49.52	45.99	41.59	335.5	183.08	17.50	13.34
4lobed BASE=376 LOBE=265	97.67	54.68	50.36	47.74	43.54	337.7	156.92	17.41	13.26
Ring1,4 lengths modified	105.2	53.71	49.02	45.57	44.11	326.6	174.60	17.52	13.33
Rings diameter modified	104.1	53.44	52.66	49.32	45.32	327.9	152.64	17.53	13.34
Overlap Increased	104.9	56.03	50.32	47.20	42.21	330.2	167.81	17.41	13.25
Diameter & Overlap Modified	104.5	53.13	50.59	47.29	43.19	329.4	180.73	17.48	13.26
6 lobed BASE=440 LOBE=183	79.58	52.13	49.53	48.19	44.19	347.0	155.53	17.05	13.01
8 lobed BASE=454 LOBE=150	65.06	33.50	30.56	30.27	30.19	354.9	133.29	23.85	13.21
10 lobed BASE=462 LOBE=130	67.96	42.36	34.26	30.88	30.11	362.2	142.09	19.29	12.56

Table2: Represents the various parameters of Models

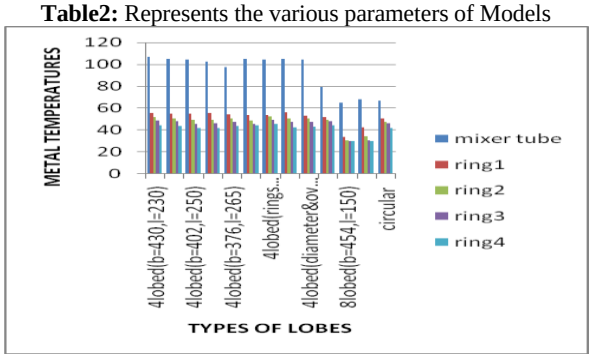

Figure8: *TYPES OF LOBES Vs METAL TEMPERATURES*

The following graph is plotted by taking the different types of lobed nozzles on X-axis and metal temperatures of mixer tube, ring1, ring2, ring3, ring4 on Y-axis.the variations of plots of metal temperature for different types of lobed nozzles can noticed from the above figure(8). From the graph it can be noticed that the metal temperature of mixer is very low in case of eight lobed nozzle and very high in case of 4lobed nozzle with base=430 and lobe=230 and coming to ring1, ring2, ring3, ring4 metal temperature it can seen that it is more in case of 4 lobed nozzle with base=430 and lobe=230 and less in case of 8 lobed nozzle. The 10 lobed nozzle metal temperatures are also less when compared with other models but high with respect to 8 lobed nozzles. All the other models are showing almost same with only slight variation but the drastic change can be seen only in 8 lobed nozzles next to it followed by 10 lobed nozzles. 8 lobed nozzles has shown maximum suction of secondary and film cooling air and the metal temperatures have attained local minimum values showing cent percent effectiveness of film cooling.

Acknowledgment:

I would like to thank my Guide **Dr.B.Balakrishna** for his time and support. In addition, I would like to thank my friends for sharing their experience in CATIA, CFD Software. Finally, I would like to thank my family for their support and putting up with me for these past few months moral and financial support during my studies

REFERENCES

1. Birk, A.M., Davis, W.R., (1988) Suppression the infrared signatures of marine gas turbines, ASME Journal of engineering for gas turbines and power, Vol.111, pp 123-129.
2. Mukherjee, D.K. (1976), Film cooling with injection through slots, ASME Transactions, Journal of engineering for power, October (1976).
3. A.M. Birk, D. VanDam, "Infra-Red Suppression for Marine Gas Turbines: Comparison of Sea Trial and Model Test Results for the DRES Ball System", ASME 92-GT-310, 1992.
4. Birk, A.M., Vandam, D., (1989) marine gas turbine infrared suppression: aero thermal design considerations, ASME 89-GT-240.
5. W.R. Davis, J. Thompson, W.R. Davis Engineering Ltd. Ottawa, Ontario, Canada. Developing an ir signature specification for military platforms using modern simulation techniques.
6. Thompson, J., Vaitekunas, D., and Birk, A.M., "IR Signature Suppression of Modern Naval Ships," ASNE 21st Century Combatant Technology Symposium, 27-30 January 1998.
7. Hoffman, K.A., and Chiang, S.T., Computational Fluid Dynamics for Engineers, in two Volumes, Engineering Education System, PO Box 20078, Wichita, KS, 67208-1078. 1993.
8. Anderson, J.D., Jr., Computational Fluid Dynamics: The Basics with Applications, McGraw-Hill, Inc., New York, 1995.
9. Hudson, R.D. "Infrared System engineering", John Wiley and Sons, 1969, ISBN 471 41850.
10. H.K.Versteeg,and W.Malalasekera, "An Introduction to Computational Fluid Dynamics" The Finite Volume Method".
11. Holeman JP, "Heat Transfer", McGraw Hill Publication.
12. J. Morin, F. Reid, and D. Vaitekunas, "SHIPIR: a model for simulating infrared images of ships at sea", SPIE 2223, 1994.
13. D.A. Vaitekunas, K. Alexan, O.E. Lawrence, and F. Reid, "SHIPIR/NTCS: a naval ship infrared signature countermeasure and threat engagement simulator", SPIE 2744, pp.411-424, 1996.
14. D.A. Vaitekunas and D.S. Fraedrich "Validation of the NATO-standard ship signature model (SHIPIR)", SPIE 3699, 1999.
15. L.F. Galle, H.M.A. Schleijpen, "Ship Infrared (IR) Signatures (Ship Survivability Part II)", article submitted to ASNE "Naval Engineers Journal", February 1997.
16. A.N. de Jong, "IR Detection of Ships during MAPTIP", Procedings NATO- IRIS Vol. 41, No. 3, 1996.
17. D.A. Vaitekunas, K. Alexan, O.E. Lawrence, F.Reid, "SHIPIR/NTCS: a naval ship infrared signature countermeasure and threat engagement simulator", SPIE Proceedings from "Infrared Technology and Applications XXII", Volume 2744, 1996.
18. H.M.A. Schleijpen, "Evaluation of infrared signature suppression of ships" TNO Physics & Electronics Laboratory, the Netherlands.
19. M.D. Mermelstein, "Midwave and long-wave infrared radiance and clutter at the ocean-sky horizon", Optical Society of America, 0146-9592 /94/181385-03, March 1994.
20. A.N. de Jong, "Ship Infrared Vulnerability Experiment (SIVEX)", NATO Panel 4 - Research Group 5, technical report AC/243 (Panel 4) TR/8, April 1992.